Hindawi
International Journal of Antennas and Propagation
Volume 2023, Article ID 5281547, 8 pages
https://doi.org/10.1155/2023/5281547

Research Article

An Improved GOMP Sparse Channel Estimation for Vehicle-to-Vehicle Communications

Xin Chen,[1,2] **Xudong Zhang**,[1] **Yaolin Zhu**,[1] **and Ruiqing Ma**[2]

[1]*School of Electronic Information, Xi'an Polytechnic University, Xi'an 710048, Shaanxi, China*
[2]*College of Automation, Northwest University of Technology, Xi'an 710129, Shaanxi, China*

Correspondence should be addressed to Xin Chen; chenxin@xpu.edu.cn

Received 27 March 2023; Revised 14 August 2023; Accepted 10 October 2023; Published 6 November 2023

Academic Editor: Chien-Jen Wang

Reliable channel estimation is critical for wireless communication performance, especially in vehicle-to-vehicle (V2V) communication scenarios. Aiming at the major challenges of channel tracking and estimating as the highly dynamic nature of vehicle environments, an improved generalized orthogonal matching pursuit (iGOMP) is proposed for V2V channel estimation. The iGOMP algorithm transforms the channel estimation problem into a sparse signal recovery problem and replaces the classical inner product criterion with the Dice atom matching criterion. Additionally, the atomic weak progressive selection method is integrated to avoid the suboptimal selection of atoms from the redundant dictionary using the inner product criterion. The proposed iGOMP method can achieve optimal channel estimation by iterating feedback results. Simulation results demonstrate that the iGOMP method has superior estimation accuracy, mean square error (MSE), and bit error rate (BER) performance compared with traditional channel estimation methods in V2V communications.

1. Introduction

With the continuous deployment of 6G artificial intelligence technology in applications such as autonomous driving and the Internet of vehicles (IoV), the application of IoV technology has evolved from initial information entertainment to safety guarantee and efficiency improvement under the conditions of vehicle-to-vehicle (V2V) and vehicle-to-infrastructure (V2I) information interaction [1–3]. In V2V communication systems, both the transmitter (Tx) and the receiver (Rx) are in a moving state, and the antenna height is low, making it easily blocked by scatterers. When switching to different scenarios, the wireless channel shows nonwide sense stationary uncorrelated scattering (non-WSSUS) fading characteristics [4–6]. Moreover, researchers have experimentally demonstrated that V2V channels have sparse properties in V2V environments [7, 8]. Reliable information transmission is closely related to the transmission characteristics of the wireless channel, and since the wireless channel in V2V environments usually presents highly dynamic characteristics, accurate estimation of the channel impulse response (CIR) is crucial for subsequent equalization and demodulation. Therefore, the accuracy of channel estimation determines reliable information transmission in V2V environments [9, 10]. Due to the combined effects of multipath fading and Doppler shift, high-speed scenarios exhibit both time/frequency selective fading and time-varying nonstationary channel characteristics in the time domain, which can significantly affect the latency communication in IoV scenarios [11–13].

In V2V communications, the channel is always sparse, which means that the multipath channel has a large delay spread, but its energy is mainly concentrated in a few paths, with fewer components in other paths [14]. In light of this sparsity characteristic, compressed sensing technology can be used to achieve good channel estimation performance through a number of observations, with lower complexity than traditional algorithms. The authors of [15] investigate the iterative stop criterion for sparsity estimation, as CS-based sparse signal detections require accurate sparsity information. By analyzing the residual energy, the Tx can determine whether active pilot components are included in the residual, preventing an increase in the complexity of JMPA decoding due to excessive false detections. The greedy algorithm is a common algorithm in compressive sensing reconstruction, with lower complexity compared to convex optimization methods, making it more widely used. Orthogonal matching pursuit (OMP) is a commonly used representative greedy algorithm for estimating sparse channels. However, its iteration time increases when the sparsity level is high [16]. In [17], authors proposed a generalized orthogonal matching algorithm (GOMP), which selects a few atoms with the largest product with the residual. The OMP algorithm is a special GOMP algorithm. Compared with the OMP algorithm, GOMP has a higher computing speed. GOMP uses simple multiatom selection for the OMP algorithm, meaning that after calculating the inner product of the residual and the unselected atoms using the current residual approximation criterion, M atoms with the largest inner product are selected in turn. This method of selecting M optimal multiatom selection methods is simple to implement, with less calculation time than that of the OMP algorithm, and improved reconstruction performance compared to the OMP algorithm. In this paper, the algorithms are applied to V2V sparse channel estimation, but the minimum MES and BER are slightly worse. In [18], authors proposed a sequential processing algorithm for unknown sparsity, which increases the sparsity by sampling the signal until the stopping criterion is met. In [19], authors proposed a decision-guided solution to improve the equalization performance by utilizing the sparsity of the arrival angles and reconstructing the channel using the block orthogonal matching pursuit algorithm (BOMP), but at a high computational complexity. Although these solutions improve the accuracy of channel estimation, the sparsity of the channel is usually difficult to obtain, and previous literature often assumes that the channel sparsity is known before performing channel estimation.

Motivated by the aforementioned, an iGOMP algorithm is proposed in this paper, which involves postprocessing the iterative results obtained by the GOMP algorithm and removing redundant atoms. Theoretical analysis and simulation results show that although both the MSE and BER of the GOMP algorithm are slightly worse than those of the OMP algorithm, the former has a shorter running time and lower computational complexity. Compared with the GOMP algorithm, the iGOMP algorithm produces better MSE and BER performance. The remaining sections of this paper are organized as follows. Section 2 presents the system and channel model. Section 3 describes the proposed improved generalized orthogonal matching pursuit algorithm. Section 4 compares the performance of the proposed method with traditional methods in the V2V channel. Finally, the conclusion is presented in Section V.

2. System and Channel Model

2.1. System Model. The rapid movement of the Tx and Rx in V2V scenarios causes a Doppler frequency shift, resulting in a frequency offset of the subcarriers in the OFDM system. This offset destroys the orthogonality of the subcarriers and significantly affects the system's performance.

Assuming that the OFDM system has N subcarriers, of which P subcarriers are allocated for pilot symbol transmission, and each subframe consists of I OFDM symbols, the resource element of the $i-$ th transmitted OFDM symbol on a subcarrier can be denoted as $s_i = [s_i(0), \cdots, s_i(n), \cdots, s_i(N-1)]^T$. When performing s_i OFDM modulation through inverse fast Fourier transform (IFFT), it can be expressed as follows:

$$S_i = F^H s_i, \tag{1}$$

where S_i represents the transmitted time domain signal, F represents the DFT transformation matrix of the point $([F]_{n,k} = 1/\sqrt{N} \exp(-j2\pi/N\mathrm{kn}))$, and $(\cdot)^H$ represents the conjugate transpose, and then, the OFDM transmission model is defined as follows:

$$Y_i = H_i s_i + z_i, \tag{2}$$

where $Y_i = [y_i(0), y_i(1), \cdots, y_i(N-1)]^T$ is the vector of the received signal at $i-$ th OFDM symbol in the time domain, z_i is additive complex white Gaussian noise of the channel, and H_i denotes the CIR matrix on the $i-$ th OFDM symbol, which could be defined as follows:

$$H_i = \begin{bmatrix} h_i(0,0) & 0 & \cdots & 0 & h_i(0,1) \\ h_i(1,1) & h_i(1,0) & \cdots & 0 & h_i(1,2) \\ \vdots & \vdots & \vdots & \vdots & \vdots \\ h_i(L-1,L-1) & 0 & \cdots & h_i(N-2,0) & 0 \\ 0 & 0 & \cdots & 0 & h_i(N-1,0) \end{bmatrix}, \tag{3}$$

where $h_i(k,l)$ is the $k-$ th CIR sample point on $l-$ th tap at $i-$ th OFDM symbol.

After FFT demodulation at the receiving end, Y is obtained, which is expressed as follows:

$$Y_i = F_i h_i F^H X_i + F z_i = H_i X_i + Z_i, \tag{4}$$

where $Y_i = [Y_i(0), Y_i(1), \cdots, Y_i(N-1)]^T$ and $X_i = [X_i(0), X_i(1), \cdots, X_i(N-1)]^T$ are the Tx and Rx signals in the frequency domain, respectively, and Z_i is the expression of the additive Gaussian noise vector z_i in the frequency domain.

Let Q be a $P \times N$ dimensional pilot selection matrix obtained by selecting P rows from an $N \times N$ dimensional identity matrix corresponding to the pilot positions. The received signal at the pilot positions can be expressed as follows:

$$Y_P = X_P F_P h_P + Z_P, \tag{5}$$

where Y_P represents the corresponding signal received at the receiver for the pilot signal, $X_P = \mathrm{QXQ}^{-1}$ represents the signal transmitted for the pilot, and Z_P represents the noise in the channel. For the receiver, Y_P, X_P, and Z_P are all known signals.

The process of recovering h based on (5) can be modeled as a sparse signal reconstruction problem in the presence of noise. Therefore, compressive sensing techniques can be employed to reconstruct the sparse vector h. Subsequently, the frequency-domain channel impulse response samples can be obtained by calculating $H_p = F_p \times h_p$, where H_p represents the samples of the channel frequency-domain impulse response.

2.2. V2V Channel Model. The channel characteristics of V2V communication are scene-dependent. Figure 1 depicts a typical V2V communication scenario in an urban area, where the multipath effect is significant due to the presence of near and far scatterers such as buildings and vehicles.

In this paper, the tapped delay line (TDL) model is used as the V2V channel model, and the expression of CIR is derived as follows:

$$\begin{aligned} h(t,\tau) &= \sum_{l=0}^{L-1} \alpha_l(t) \cdot \delta(\tau - \tau_l(t)) \\ &= \sum_{l=0}^{L-1} \beta_l(t) \cdot \exp\left(j2\pi f_{D,l} t\right) \cdot \delta(\tau - \tau_l(t)), \end{aligned} \tag{6}$$

where $\alpha_l(t) = \beta_l(t) \cdot \exp(j2\pi f_{D,l} t)$ reflects the fading characteristics, $\beta_l(t)$ represents the amplitude of the $l-$th path, $f_{D,l}$ represents the Doppler shift of the $l-$th path, $\tau_l(t)$ denotes the time delay of the $l-$th path, respectively, and L is the number of paths in the V2V channel. In the TDL model, each tap corresponds to a multipath, and its fading amplitude statistics and Doppler spectrum determine the main characteristics of the channel under a specific scenario. If a delay tap corresponds to a non-line-of-sight (NLoS) component, the tap follows Rayleigh fading; if a delay tap corresponds to a line-of-sight (LoS) component, the tap is modeled using Rician fading.

The authors of [20] provide specific channel parameters for six V2V communication scenarios. Therefore, the V2V-urban canyon oncoming (V2V-UCO) scenario is studied, and the specific channel parameters are shown in Table 1.

3. Sparse Channel Estimation Algorithm Based on Improved GOMP

3.1. Generalized Orthogonal Matching Algorithm (GOMP). The purpose of the GOMP algorithm, based on multiatom selection, is to reduce the computational complexity and running time of the OMP algorithm. The atomic selection principle of the GOMP algorithm is to choose M atoms with the largest inner product of the residual from all the unselected atoms, which extends the OMP algorithm. The OMP algorithm is a special case of GOMP ($M=1$), and the algorithmic pseudocode is as follows.

3.2. Atomic Weak Selection. In V2V communications, it is often difficult to apply the GOMP algorithm since it requires knowledge of the signal sparsity. To address this issue, the atomic weak selection method can be used. This method does not select atoms based on their correlation but instead sets a threshold and groups atoms larger than the threshold into atomic sets while discarding the remaining atoms. The residuals are then updated and stacked until the stopping condition is satisfied.

The weak selection criteria for atoms are shown as follows:

$$\left\{ i \left| \left| u_j \right| \geq a. \max_j \left| u_j \right| \right. \right\}. \tag{7}$$

When the observation matrix is a Gaussian matrix, threshold parameter m is set a value within the range from 2 to 3, where δ_t represents the noise power, and the number of columns in the observation matrix is denoted by N.

The elements in the inner product column that satisfy the selection criterion of the atoms are added to the atom set, and their column index is added to the index set, by computing the inner product between the current residual and the recovery matrix. The weak selection method of atoms allows the process to be unrestricted by sparsity and can adjust the number of selected atoms according to the inner product value between the current residual and the recovery matrix. This effectively avoids the problem of selecting too many or incorrect atoms in advance and improves the stability of the algorithm.

3.3. DICE Guidelines. The classical channel estimation algorithm based on compressed sensing typically measures the similarity between vectors using the inner product criterion. However, using this method to represent correlation has certain drawbacks. During signal recovery, some similar atoms in the observation matrix can impact the matching of the signal residual, ultimately reducing the accuracy of the signal recovery.

Therefore, selecting an appropriate measurement method to screen the atoms in the support set has become a critical factor that affects the quality of the signal reconstruction algorithm. To address this issue, the measurement criterion has been improved. Specifically, the Dice coefficient matching criterion is now used in the first stage of atom screening. The Dice coefficient matching criterion expresses the similarity between vectors β and λ as follows:

$$\mathrm{Dice}(\beta,\lambda) = \frac{2\sum_{i=1}^{n} \beta_i \lambda_i}{\sum_{i=1}^{n} \beta_i + \sum_{i=1}^{n} \lambda_i^2}. \tag{8}$$

Through a comparative analysis of the mathematical expressions of the dot product criterion and the Dice coefficient matching criterion, it can be inferred that the denominator calculation method used in the dot product criterion can compromise the inherent characteristics of the vectors, making it challenging to differentiate between similar atoms. Conversely, the calculation method employed in the Dice coefficient matching criterion can effectively address this issue. Therefore, the Dice criterion can identify more appropriate atoms and improve the accuracy of reconstruction.

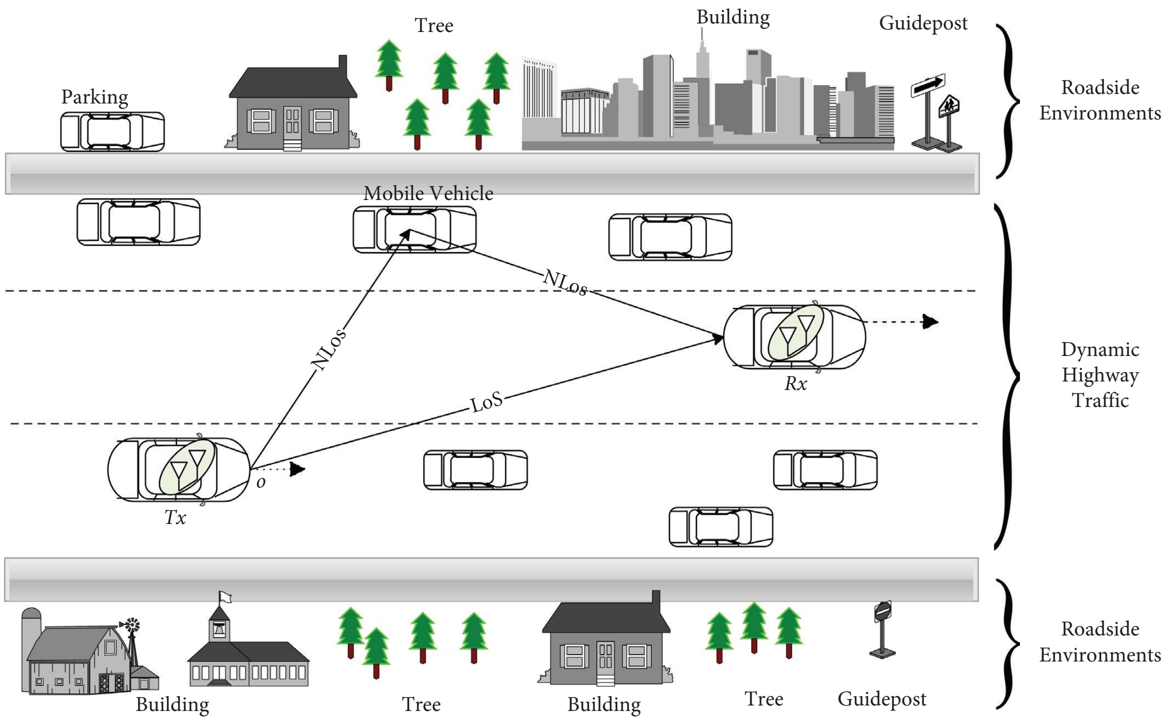

Figure 1: V2V communication scenarios in urban.

Table 1: Channel parameters for V2V communication scenarios.

Parameters	V2V-UCO
Transceiver distance (m)	100
Number of taps	5
Fading distribution	Rician (1)/Rayleigh (4)
Latency (100 ns)	[0, 1, 2, 3, 4]
Gain (dB)	[0, −10, −17,8, −21,1, −16,3]
Rice coefficient K (dB)	4.0
Maximum Doppler shift (Hz)	400~500
LOS Doppler shift (Hz)	1263
Fading spectrum shape	[R, R, R, R, J]

3.4. Improved Generalized Orthogonal Matching Algorithm (iGOMP). The GOMP selects a few atoms with the highest product with the residual at each iteration, which can lead to the selection of incorrect atoms. Moreover, the GOMP algorithm can accurately reconstruct the signal only when the sparsity of the channel is known in advance, which is not always feasible in real V2V environments. To solve the technical problems, an improved version of the GOMP algorithm, known as the iGOMP, has been proposed for V2V channels [22, 23]. This algorithm accurately estimates channel information even when sparsity is unpredictable and achieves a low BER as shown in Table 3.

4. Simulation Results and Analysis

To evaluate the performance of the iGOMP algorithm in V2V scenarios, we conduct a systematic simulation of the proposed iGOMP V2V channel estimation algorithm on the MATLAB R2016a platform, as specified in Table 4. Specifically, we compare the performance of the iGOMP algorithm against five traditional channel estimation algorithms (LS, OMP, SAMP, GOMP, and iGOMP) in the V2V-UCO scenario. BER and MSE are used as performance metrics for channel estimation quality.

Comparing the simulation results of the channel estimation algorithm in the V2V-UCO scenario, it is found that the accuracy of the channel estimation based on the OMP, SAMP, GOMP, and iGOMP algorithms is higher than that of the LS algorithm under the same SNR. This is due to the fact that the V2V channel estimation algorithm based on compressed sensing takes into account the sparseness of the channel and can obtain a better estimation effect by using fewer pilots. Since the reconstruction performance of compressive sensing is relatively low SNR, reconstruction is not meaningful in this range, and therefore, the variation range of SNR is set to 5~30 dB. The analysis indicates that, under the same number of pilots, the MSE of each method decreases with the increase of SNR. Base channel estimation on the matching pursuit greedy method takes into account the sparse characteristics of the channel, and its MSE performance is significantly better than that of LS. For instance, OMP has an SNR peak gain of about 10 dB compared to LS. Figure 2 compares the MSE performance of different methods in various speed environments. The proposed method has an SNR peak gain of about 15 dB compared to OMP and an SNR peak gain of about 5 dB compared to SAMP, which demonstrates that the method proposed in this paper improves the performance based on MSE performance of channel estimation for typical matching pursuit-like greedy methods. There are main reasons for this: first, the method proposed in this paper incorporates the

Table 2: GOMP algorithm pseudocode [21].

Input: measure matrix Φ, sample vector Y, channel sparsity K, atoms M;
Output: A K-sparse approximation $\widehat{h}$ of the input signal;
Initialization: support sets $F_0 = \varnothing$, residual $r_0 = Y$, iterations $t = 1$;
(1) Calculate $u = \text{abs}[A^T r_{t-1}]$, find the u values with the largest measurement matrix and residuals by M, $t = t + 1$, and get the candidate $A_t = A_{t-1} \cup J_0$;
(2) Calculate $\widehat{h}_t = \text{argmin}\|Y - \Phi u\|$, take the M mark corresponding to the largest value into a collection F, and calculate residual $r_t = Y - \Phi_F \Phi_F^+ \widehat{h}$;
(3) Determine $t \le \min(K, M/S)$, if meeting, executive 1, if not meeting, stop iterating and output $\widehat{h}$; after cycle steps 1–3, it will output h sparse approximation, namely $\widehat{h}$

Table 3: iGOMP algorithm pseudocode [22].

Input: measure matrix Φ, sample vector Y, step S, channel sparsity K, atoms M;
Output: A K-sparse approximation $\widehat{h}$ of the input signal;
Initialization: support sets $F_0 = \varnothing$, residual $r_0 = Y$, iterations $t = 0$, $L = M$;
(1) Calculate based on DICE criteria, find the u values with the largest measurement matrix and residuals by M, which corresponding column vector with values greater than the threshold $Th = \alpha \max\{\text{abs}(u)\}$ is recorded as set α_J;
(2) Get the candidate $F = F_{t-1} \cup J_0$, $A_F = \{a_j\}$;
(3) Calculate $\widehat{h}_t = \text{argmin}\|Y - \Phi u\|$, take the M mark corresponding to the largest value into a collection F, and calculate residual $r_t = Y - \Phi_F \Phi_F^+ h$;
(4) Determine $\|r_{t-1}\|_2 \le \varepsilon_1$, if meeting, executive 5, if not meeting, executive 6;
(5) Determine $\|r_{t-1}\|_2 \le \varepsilon_2$, if meeting, change the support set $L = L + 1$, $t = t + 1$, executive 1
(6) Set $t = t + 1$, $L = t * S$, $\text{F}_t = F$, $r_t = r$, $t = t + 1$;
(7) Determine $t \le \min(K, M/S)$, if meeting, executive 1, if not meeting, stop iterating and output $\widehat{h}$, after cycle steps 1–6, it will output h sparse approximation, namely $\widehat{h}$

Table 4: List of key V2V channel parameters in simulating.

Parameter name	Value
Channel model	TDL
Carrier frequency	5.9 GHz
System bandwidth	10 MHz
Observation matrix	Gaussian random matrix
Total number of subcarriers	128
Cyclic prefix	16
Channel additive noise	Gaussian noise
Doppler shift	400 Hz
Speed v_t	60km/h
Speed v_r	120km/h
Modulation	QPSK
Pilot format	Comb pilot
SNR (dB)	5–30
Sparsity (OMP/GOMP)	10
Step size	$S = 2$
Threshold	$\varepsilon_1 = 10^{-5}, \varepsilon_2 = 0.2 \times 10^{-5}$

multiatom selection of GOMP and the backtracking idea of SAMP into OMP, which enables efficient and precise screening of atoms by providing the ability to delete previously selected atoms and ensuring optimality at each iteration. This significantly improves the performance of the GOMP algorithm. Second, the use of double thresholds addresses the problem of fixed step size in GOMP. At each iteration, the energy difference of the reconstructed signal is evaluated to determine whether it is close to ε_2. If it approaches ε_2, a small step size is adopted to gradually approach the estimated value and improve the reconstruction accuracy. This leads to an improvement in the performance of channel V2V estimation.

Figure 3 illustrates the BER performance of various channel estimation algorithms at different speeds. The iGOMP channel estimation algorithm proposed in this paper demonstrates superior performance at different speeds. As the SNR increases, the channel estimation based on the matching pursuit greedy method and LS shows a downward trend in BER, but the former displays a more pronounced decline. This is due to the fact that, at the same SNR, the matching pursuit greedy method has better channel estimation performance than LS. When the SNR increases to 30 dB, the channel estimation based on the matching pursuit greedy method and LS gradually becomes stable since the noise is relatively low at this point, and the performance of each method relies mainly on its own estimation accuracy. Furthermore, the method proposed in this paper has an SNR peak gain of 15 dB relative to OMP and a 5 dB SNR gain relative to SAMP in terms of BER performance. At a velocity of 120 km/h, LS, OMP, GOMP, and SAMP have lower limit as SNR increases, whereas the iGOMP algorithm continues to maintain excellent performance. The main reason for the significant improvement in channel estimation performance is that in low-speed environments, the CIR changes very slowly within a single symbol time unit. However, in high-speed scenarios, the proposed algorithm is able to adaptively estimate the real sparsity of the channel, resulting in greatly improved channel estimation performance.

Figure 4 compares the performance of iGOMP with different step lengths in the V2V-UCO scenario. As shown in the figure, when the step size is set to $S = 2$, iGOMP achieves better BER and MSE performance compared with

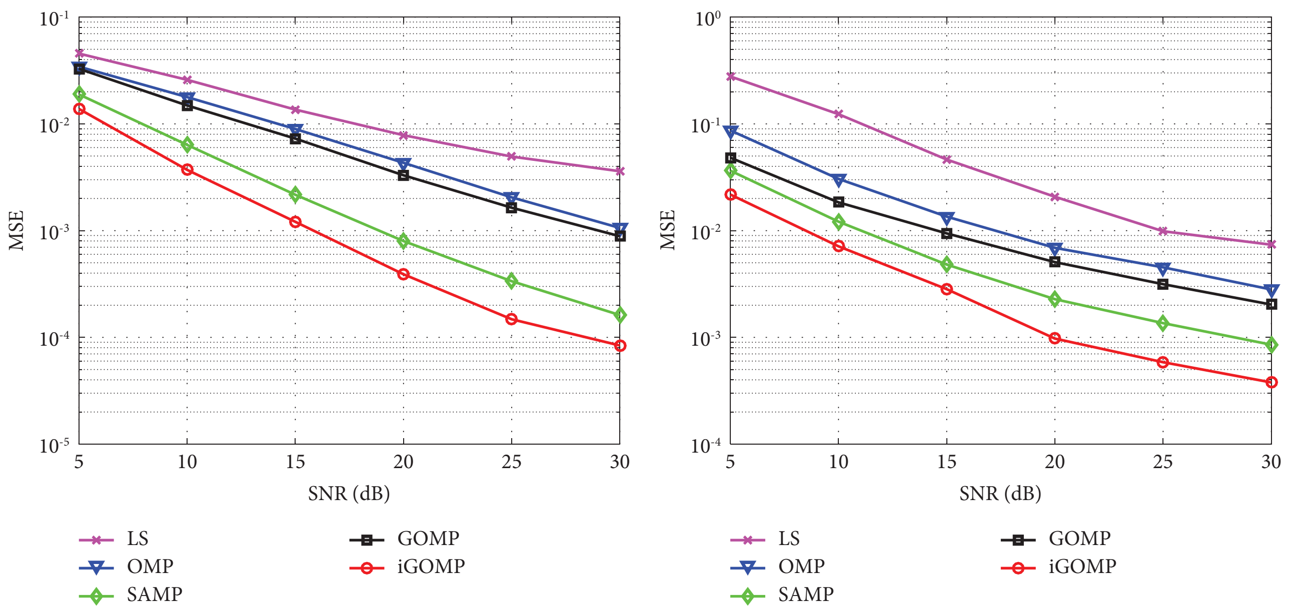

(a) (b)

Figure 2: MSE comparison of each channel estimation algorithm in V2V-UCO scenario. (a) MSE performance of each algorithm when moving speed is 60 km/h and (b) MSE performance of each algorithm when moving speed is 120 km/h.

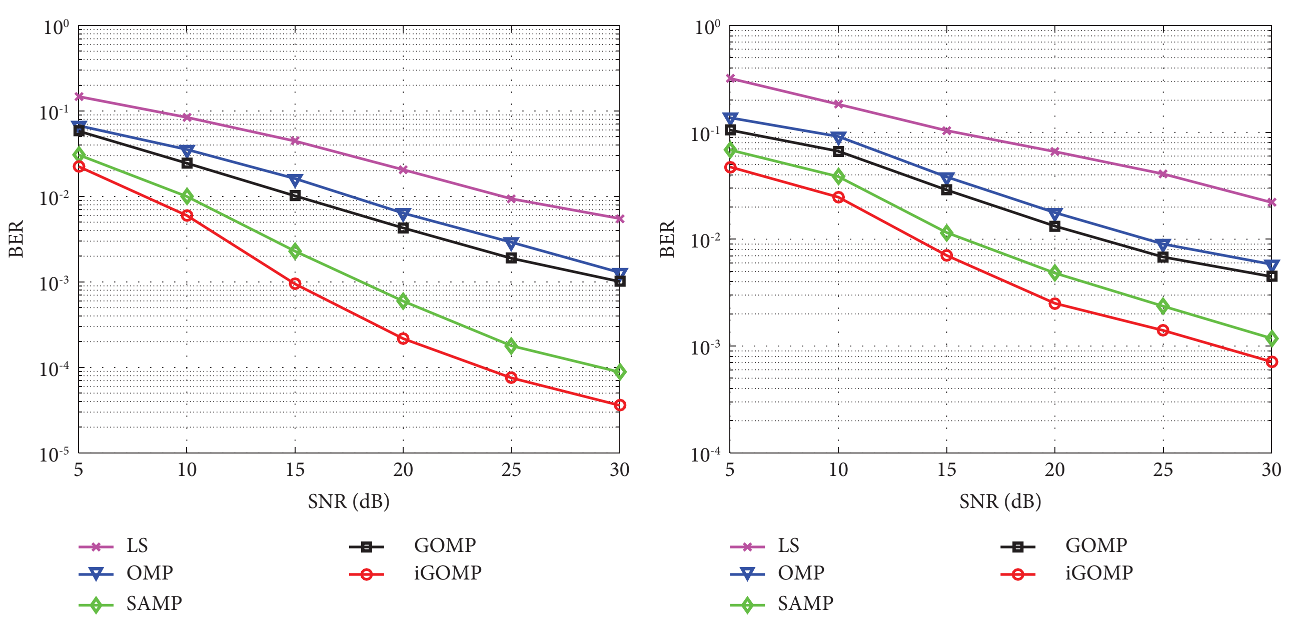

(a) (b)

Figure 3: BER comparison of each channel estimation algorithm in V2V-UCO scenario. (a) BER performance of each algorithm when moving speed is 60 km/h and (b) BER performance of each algorithm when moving speed is 120 km/h.

$S = 3$ and $S = 5$. When the MSE is set to 1×10^{-3}, there is approximately a 5 dB gain compared with $S = 2$ and $S = 3$ about 9 dB gain compared with $S = 5$. Since different step sizes can affect the performance of the algorithm, if the initial step size is large, the support set will quickly expand. Although the signal reconstruction rate will increase, the accuracy of the reconstruction will decrease. If a smaller initial step size is set, the signal can be reconstructed more accurately, thereby improving the accuracy of the algorithm.

Table 5 shows a comparison of the runtime performance for the aforementioned methods in a single complete channel estimation at SNR = 30dB. The simulation tool used

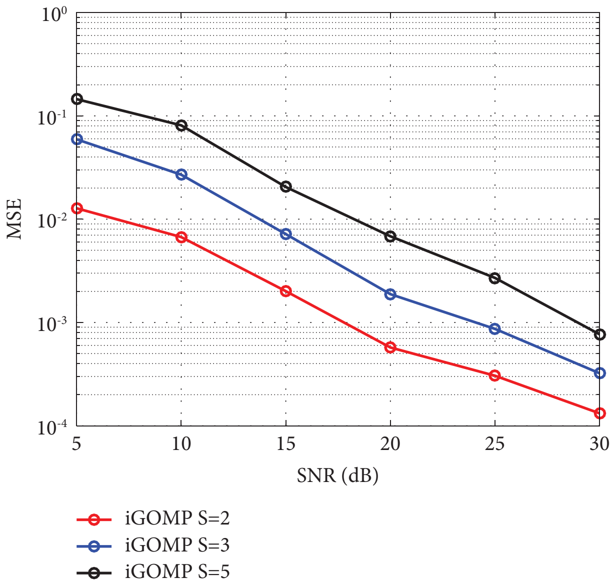

(a)

(b)

Figure 4: Comparison of MSE and BER performance of iGOMP algorithm under different step lengths. (a) MSE comparison of iGOMP algorithm and (b) BER comparison of iGOMP algorithm.

Table 5: Comparisons of running time among different algorithms.

Algorithm	Running time (s)
OMP	0.1021
GOMP	0.0352
SAMP	0.1388
iGOMP	0.1506

Table 6: Complexity comparisons among different algorithms.

Algorithm	Time complexity
LS	$O(N)$
OMP	$O(\mathrm{KPN})$
GOMP	$O(\mathrm{KPN})$
SAMP	$O(\mathrm{KPNlg}\,S/S)$
iGOMP	$O(\mathrm{KPNlg}\,S/S)$

was MATLAB 2016a, and the computer was equipped with a 2.8 GHz, Intel i5 CPU, 8 GB of memory, and the Windows 10 operating system. Analysis shows that the iGOMP algorithm has a slightly longer average runtime than the other methods due to its more complex and numerous atomic screening steps and the introduction of dual thresholds to set the stopping iteration conditions.

Table 6 presents the comparisons of the complexities of different algorithms in two aspects: the number of multiplication operations and the time complexity. It can be observed from Table 6 that the LS algorithm has the lowest complexity. Compared with the OMP algorithm, the SAMP algorithm has only one more logarithmic order, which is lg S. The reason for this is that the SAMP algorithm approximates sparsity for reconstruction, which increases complexity, but its step size is S much smaller than N, so its impact on complexity is limited. Therefore, the complexity of the proposed algorithm is within a tolerable range for research. The time complexity of the iGOMP algorithm and the SAMP algorithm is the same, and they have the same order of magnitude as a whole.

5. Conclusion

To further improve the communication quality in the V2V environments of the vehicular communications, this paper proposes an iGOMP algorithm of sparse channel estimation for diverse and dynamic V2V propagation environments. The algorithm integrates the weak selection method of the Dice criterion to select atoms and improves the reconstruction accuracy of the estimated value by gradually approximating it using a small step size. This approach can effectively address the problem in traditional algorithms where the inner product criterion cannot select the optimal atom from a redundant dictionary, thereby enhancing the stability of the algorithm. Simulation results show that the proposed algorithm has higher estimation accuracy compared with LS, OMP, SAMP, and GOMP. At a fixed SNR, the BER and MSE of algorithms were improved, effectively enhancing the performance of V2V channel estimation. Although the proposed method has slightly higher complexity and runtime compared with other methods mentioned aforementioned, it is still within an acceptable range and proves that the algorithm performance is affected by different step sizes and V2V communication scenarios.

Data Availability

The data will be made publicly available upon reasonable request through the corresponding author.

Conflicts of Interest

The authors declare that they have no conflicts of interest.

Acknowledgments

This work was supported by the Chinese Postdoctoral Science Foundation under Grant no. 2020M683562, the Natural Science Foundation of Shaanxi Province of China under Grant no. 2022JM-331, the Key Research and Development Program of Shaanxi Provincial Science and Technology under Grant no. 2023-YBGY-142, the Scientific Research Project of Shaanxi Provincial Education Department under Grant no. 23JC031, and the Science and Technology Program of Xi'an, China, under Grant no. 23GXFW0027.

References

[1] L. Zhao, H. Li, N. Lin, M. Lin, C. Fan, and J. Shi, "Intelligent content caching strategy in autonomous driving toward 6G," *IEEE Transactions on Intelligent Transportation Systems*, vol. 23, no. 7, pp. 9786–9796, 2022.

[2] H. Jiang, M. Mukherjee, J. Zhou, and J. Lloret, "Channel modeling and characteristics for 6G wireless communications," *IEEE Network*, vol. 35, no. 1, pp. 296–303, 2021.

[3] Z. Lv, L. Qiao, and I. You, "6G-Enabled network in box for Internet of connected vehicles," *IEEE Transactions on Intelligent Transportation Systems*, vol. 22, no. 8, pp. 5275–5282, 2021.

[4] X. Cheng and Y. Li, "A 3-D geometry-based stochastic model for UAV-MIMO wideband nonstationary channels," *IEEE Internet of Things Journal*, vol. 6, no. 2, pp. 1654–1662, 2019.

[5] J. R. Jaime, C. A. Gutierrez, and M. Patzold, "On the spectral moments of non-WSSUS mobile-to-mobile double-Rayleigh fading channels," in *Proceedings of the 2017 IEEE 28th Annual International Symposium on Personal Indoor and Mobile Radio Communications*, pp. 1–6, Montreal, Canada, October 2017.

[6] Y. Li, R. He, and S. Lin, "Cluster-Based Non-stationary Channel Modeling for Vehicle-to-Vehicle Communications," *IEEE Antennas & Wireless Propagation Letters*, vol. 16, pp. 1–4, 2016.

[7] X. Shen, Y. Liao, X. Dai, M. Zhao, K. Liu, and D. Wang, "Joint channel estimation and decoding design for 5G-enabled V2V channel," *China Communications*, vol. 15, no. 7, pp. 39–46, 2018.

[8] J. Ma, S. Zhang, H. Li, F. Gao, and S. Jin, "Sparse bayesian learning for the time-varying massive MIMO channels: acquisition and tracking," *IEEE Transactions on Communications*, vol. 67, no. 3, pp. 1925–1938, 2019.

[9] W. Hou, R. S. Z. Yiin, and C. K. Goh, "Metronidazole induced encephalopathy: case report and discussion on the differential diagnoses, in particular, Wernicke's encephalopathy," *Journal of Radiology Case Reports*, vol. 13, no. 9, pp. 1–7, 2019.

[10] X. Cheng, C. X. Wang, B. Ai, and H. Aggoune, "Envelope level crossing rate and average fade duration of non-isotropic vehicle-to-vehicle ricean fading channels," *IEEE Transactions on Intelligent Transportation Systems*, vol. 15, no. 1, pp. 62–72, 2014.

[11] R. He, C. Schneider, B. Ai et al., "Propagation channels of 5G millimeter-wave vehicle-to-vehicle communications: recent advances and future challenges," *IEEE Vehicular Technology Magazine*, vol. 15, no. 1, pp. 16–26, 2020.

[12] P. S. Bithas, G. Efthymoglou, and A. G. Kanatas, "V2V cooperative relaying communications under interference and outdated CSI," *IEEE Transactions on Vehicular Technology*, vol. 67, no. 4, pp. 3466–3480, 2018.

[13] Y. Chen, Z. Dou, and Y. Lin, "Prediction of V2V Channel Quality under Double-Rayleigh Fading Channels," in *Proceedings of the 2020 IEEE 91st Vehicular Technology Conference*, pp. 1–6, Antwerp, Belgium, May 2020.

[14] M. A. Khna, V. Jeoti, and A. M. Zakakya, "Improved pilot-based LS and MMSE channel estimation using DFT for DVB-T OFDM systems," *IEEE Symposium on Wireless Technology & Applications*, vol. 18, no. 7, pp. 120–124, 2013.

[15] M. B. Sutar and V. S. Patil, "LS and MMSE estimation with different fading channels for OFDM system," *International conference of Electronics, Communication and Aerospace Technology*, vol. 25, no. 8, pp. 740–745, 2017.

[16] Y. Wang, S. Zhou, and L. Xiao, "Sparse Bayesian learning based user detection and channel estimation for SCMA uplink systems," in *Proceedings of the 2015 International Conference on Wireless Communications & Signal Processing*, pp. 1–5, Nanjing, China, October 2015.

[17] Z. Gao, L. Dai, W. Dai, B. Shim, and Z. Wang, "Structured compressive sensing-based spatio-temporal joint channel estimation for FDD massive MIMO," *IEEE Transactions on Communications*, vol. 64, no. 2, pp. 601–617, 2016.

[18] T. V. Nguyen, T. Q. Quek, and H. Shin, "Joint channel identification and estimation in wireless network: sparsity and optimization," *IEEE Transactions on Wireless Communications*, vol. 17, no. 5, pp. 3141–3153, 2018.

[19] Y. Zhan, W. Zhang, H. Deng, and Sparsity-Aware, "Direct equalization of time-varying channels for V2V communications," *IEEE Wireless Communications Letters*, vol. 10, no. 2, pp. 387–391, 2021.

[20] D. W. Matolak and Q. Wu, "Channel Models for V2V Communications: A Comparison of Different Approache," in *Proceeding of the 5th European Conference on Antennas and Propagation*, pp. 2891–2895, Rome, Italy, April 2011.

[21] J. Wang, S. Kwon, and B. Shim, "Generalized orthogonal matching pursuit," *IEEE Transactions on Signal Processing*, vol. 60, no. 12, pp. 6202–6216, 2012.

[22] S. Qian, J. Bai, and J. Nie, "An improved gOMP channel estimation method for underwater MIMO optical communication," in *Proceedings of the 2022 International Conference on Measuring Technology and Mechatronics Automation*, pp. 866–869, Changsha, China, October 2022.

[23] J. Wang, S. Kwon, P. Li, and B. Shim, "Recovery of sparse signals via generalized orthogonal matching pursuit: a new analysis," *IEEE Transactions on Signal Processing*, vol. 64, no. 4, pp. 1076–1089, 2016.